QUANTUM MOLECULAR DYNAMICS SIMULATION OF THERMALLY ACTIVATED DELAYED FLUORESCENCE

NURULFASIHAH BINTI AZHAR

SIB170013/17106743

DEPARTMENT OF PHYSICS

FACULTY OF SCIENCE

UNIVERSITY OF MALAYA

KUALA LUMPUR

2020/2021

QUANTUM MOLECULAR DYNAMICS SIMULATION IN THERMALLY ACTIVATED DELAYED FLUORESCENCE

ABSTRACT

Last few decades, smartphones and flat televisions have been commercialized globally. The development in technology has seen a rapid progress with a lot of breakthroughs in science and engineering. Organic light-emitting diodes (OLEDs) has proven to be a very beneficial with the emergence of a flexible and transparent display. Thermally activated delayed fluorescent (TADF) molecule is a relatively new materials for OLED that is promising with its advantages in efficiency and long-lifetime performance. In this work, the efficiency of the TADF molecule is studied from the conformational perspective at different temperatures. The material used is 3-(9,9-dimethylacridin-10(9H)-yl)-9H-xanthen-9-one (ACRXTN). The results from the simulations will be analysed. The simulation involved ACRXTN that is embedded in a Zeonex as a host and single molecule in vacuum. Full Quantum Molecular Dynamics (QMD) simulation and machine learning accelerated QMD are used to study the interactions and Anaconda software. From the results, the TADF molecule is weakly affected by the different temperatures.

ACKNOWLEDGEMENT

First and foremost, I want to offer my greatest and sincerest gratitude to God, the Almighty for His blessings, wisdom, and strength that He has bestowed upon me and the peace of mind that has been granted for me to be able to finish this project. Not to be forgotten, deepest gratitude to my beloved mother for her love support and encouragement including my brother which is I am highly indebted for his helps in programming for my better understanding.

It is a genuine pleasure for my part to be able to express my utmost gratitude and special thanks to my final year project supervisor, lecturer, and guide who gave me the chance to undertake this project, Assoc. Prof. Dr Woon Kai Lin on his dedication, guidance, hard work and efforts throughout the whole journey of completing this project.

My sincerest thanks also extend to my course mates and friends who have been willingly helped me to their best of abilities when I needed it the most. I would like to express my thanks and appreciation for all those who have lend me their helping hands.

TABLE OF CONTENTS

LIST OF FIGURES

Figure 4.10 The mean along with the standard deviation as the error bar, median +/10% with 60%, 40% error bar and mode values of the dihedral angles along with their standard deviation for QMDs with accelerated machine learning against different temperatures.

Figure 4.11 The mean along with the standard deviation as the error bar, median +/10%, and mode values of the dihedral angles for full QMDs against different temperatures.

Figure 4.12 Comparison of the (a) mean with standard deviation as the error bar, (b) median +/10%, and (c) mode values between full QMD simulations and machine learning accelerated QMD simulations against different temperatures.

LIST OF SYMBOLS AND ABBREVIATIONS

ACRXTN - 3-(9,9-dimethylacridin-10(9H)-yl)-9H-xanthen-9-one

TADF – Thermally Activated Delayed Fluorescnce

QMD – Quantum Molecular Dynamics

MD – Molecular Dynamics

OLED – Organic Light Emitting Diode

ΔE_{ST} - A splitting between singlet excited state and triplet excited state.

HOMO – Highest Occupied Molecular Orbital

LUMO – Lowest Unoccupied Molecular Orbital

TD-DFT - Time-Dependent Density Functional Theory

LIST OF TABLES

CHAPTER 1: INTRODUCTION

1.1 Background

For the last few decades, many technologies that we have seen and used until the present are continuously evolving especially in light-emitting technology. Current technologies are developing very rapidly with the applications of intensive studies and for instance the organic light-emitting diodes (OLEDs) [1]. Until now, OLEDs are mainly used for display electronics and the novelty is that, in the future, flexible and transparent OLED displays are possible [2]. As OLED is increasing in multiple applications, the benefits of it are clear but there are also the weaknesses of it. With extensive research for increasing the performance of OLED, thermally activated delayed fluorescent (TADF) is the alternative compared to traditional fluorescent [1]**.**

Computer simulation is a process where mathematical modelling is used using the computer to perform a prediction of behavioural of a physical system. Due to its benefits and credibility, researchers exploited the usage of the computer simulation for many experiments. In this research, Quantum Molecular Dynamic simulation (QMDs) is being used. Generally, it is used to determine the ground state and excited state geometry, the prediction of basic optical properties, and the importance of vibrionic coupling and QMDs also performs a full quantum calculation of the electronic structure for every configuration of the atomic nuclei. In this study, full QMD and machine learning accelerated QMD are used to simulate the dihedral angles of molecules selected and the results of both simulations are compared.

1.2 Objectives of Research

1. To study the effect of temperature on the dihedral angle of donor acceptor in TADF molecule.
2. To compare the machine learning QMD with full QMD.
3. To compare probability density spread of TADF molecule in a host and in vacuum.

1.3 Scope of Thesis

This report is divided into five 5 parts where the first part – Chapter 1 generally introduce the background of this research about the application of computer simulation, QMD on TADF molecules. The second part – Chapter 2 is the literature review which is describing about the molecular design of TADF molecule, main parameters to increase the performance and previous experiments using QMD and MD simulation and their achievements. The third part – Chapter 3 describes the methodology of this study such as the TADF molecule in the host that is simulated using QMD and data extraction and analysation using Python Programming Language. The fourth part-Chapter 4 illustrates the results and discussion of the findings. Finally, the last part – Chapter 5 that summarizes and concludes the study.

CHAPTER 2: LITERATURE REVIEW

2.1 Thermally Activated Delayed Fluorescent

TADF was first observed by Perrin in 1929 but the mechanism is unknown as quantum mechanics have not been fully developed yet [**3**]. Another observation of TADF behaviour occurred in 1961 in the eosin compound which a molecular structure as shown in Figure 1 but the mechanism is not understood at all until the early 2010s where computer and ultrafast spectroscopy are powerful enough and theory of quantum mechanics as applied in molecules are advanced enough to account the observed [9,11].

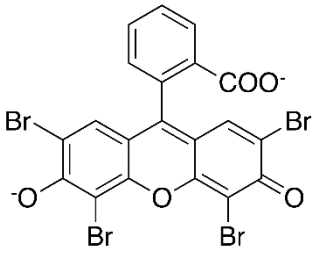

Figure 2.1. The molecular structure of eosin, 2-(2,4,5,7-tetrabromo-6-oxido-3-oxo-3*H*xanthen-9-yl)benzoate.

TADF provides the premise for all OLEDs with quantum efficiencies rivalling the transition metal-based phosphorescent devices [4]. After the high performance of TADF-OLED was being reported in 2012, many reports have emerged especially on the molecular design as one of the methods to achieve higher efficiency. The maximum internal quantum efficiency is 25% for the conventional fluorescent dopants and reaching 100% for phosphorescent emitters [4,5]. It is an arduous task to reach a higher efficiency due to the requirement and optimization of several contradicting properties.

In a simple term, TADF is a process where the surrounding thermal energy can be incorporated into non-emitting excited state of a molecule in order to transform that dark state into an emissive state. The basic mechanism of TADF can be divided into two mechanisms. The first one is being spontaneous emission where the light is emitted from the fluorescent materials by an approximate nanoseconds time scale from a singlet excited state (S_1) to a singlet ground state (S_0). The second mechanism is the delayed fluorescent where the radiative decay is delayed approximately microseconds due to the singlet states are repopulated by the triplet

excited state. Delayed fluorescence is divided into P-type and E-type as shown in Figure 2, where the P-type delayed fluorescent originated from pyrene, P-type emission originated from the triplet-triplet annihilation (TTA) which forms singlet excitons that will contribute to fluorescent emission. TTA is the formation of one singlet excision as a result of the annihilation of two triplet excitons. The E-type delayed fluorescence emerged from when the thermal energy is sufficient to excite the triplet excited back to singlet excited state due to the small splitting in between (ΔE_{ST}). This process is called reverse intersystem crossing (RISC).

Intersystem crossing is where the transformation of emissive singlet excitons into non-emissive triplet excitons. In TADF, this process is reversed. It is typically known that the electrical excitation always resulting in a ratio of 1:3 for singlet and triplet excitons due to the spin statistics. For the emission of light, only the radiative process (S_1 to S_0) can be utilized. Since 75% of the formation is in triplet, more heat is generated rather than light emission. To achieve a higher efficiency for light emission, the triplet excitons are needed to be utilized. This is done by transforming from non-emissive to emissive states through molecular engineering guided by quantum molecular physics.

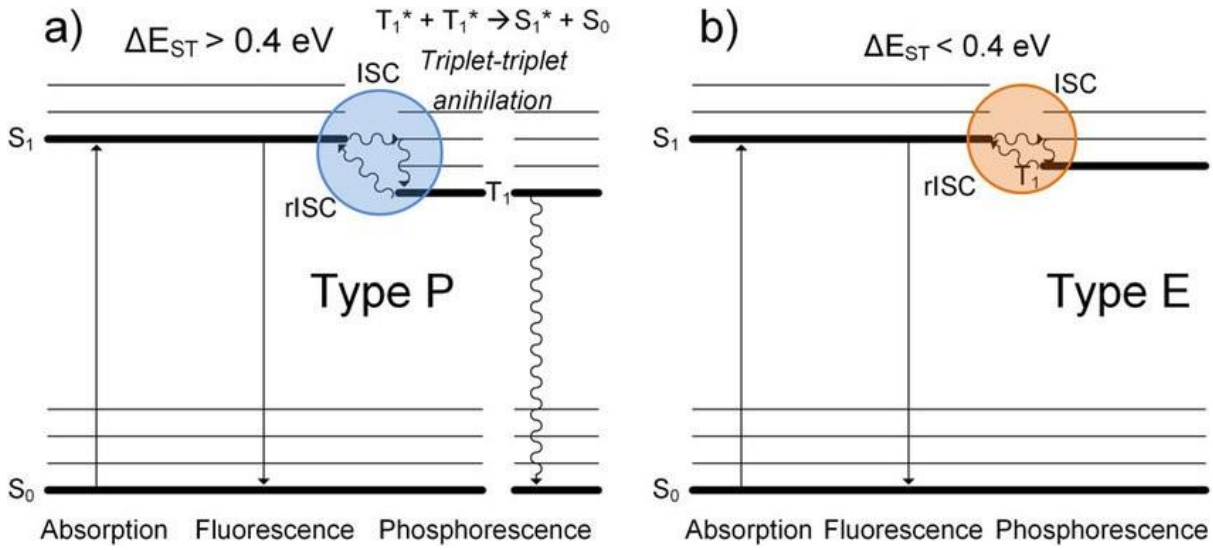

Figure 2.2. Jablonski diagram for delayed fluorescence for both types: a) P-type delayed fluorescence with triplet fusion and b) E-type delayed fluorescence [20].

The ΔE_{ST} is defined as the energy gap between the lowest singlet energy and lowest triplet energy, which is explained with the following equation,

$$E_{s1} = K + E + J \quad (1)$$

$$E_{T1} = K + E - J \quad (2)$$

$$\Delta E_{ST} = E_{s1} + E_{T1} = 2J \quad (3)$$

where K is the repulsion energy, E is the orbital energy, and J is the exchange energy decided by the overlap integral of HOMO and LUMO. To obtain a small ΔE_{ST}, it can be achieved by decreasing the overlapping of LUMO and HOMO [6]. The transition of an excited electron in organic molecules is rather complex, however, it can be summarized as in Figure 3 which illustrated the difference between fluorescence and phosphorescence.

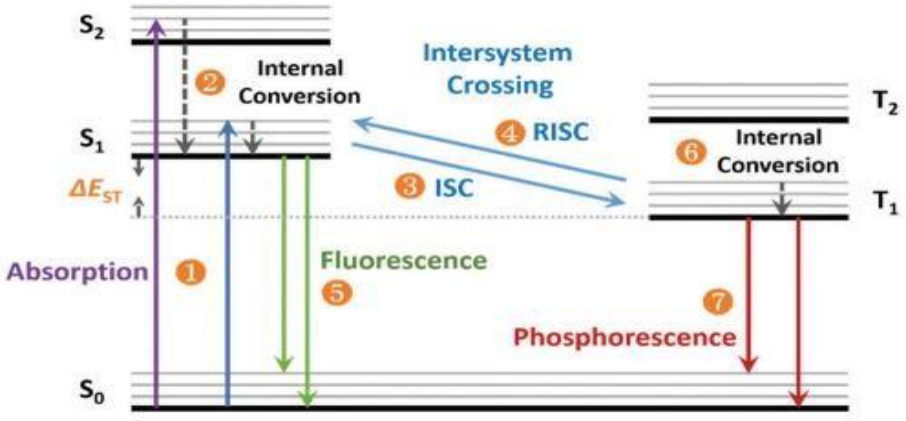

Figure 2.3. The transition process of excitons for fluorescence (**1→2→5**), phosphorescence (**1→2→3→6→7**), and TADF (**1→2→3→4→5**) in organic molecules [7].

2.2 Main Parameters of TADF

The criteria that should be set before preparing TADF emitters are donor-acceptor molecular architecture, the exact mechanism of emission is defined by the acceptor and donor linkage pattern, the dynamic rocking of acceptor and donor, conformation, thermal surrounding, and electrochemical stability, small ΔE_{ST}, and stability of triplet state. There are a few key parameters of TADF emitters which consist of ΔE_{ST}, PL quantum yield (PLQY), the emission spectrum's full width at half-maximum (FWHM), and stability. A small ΔE_{ST} is needed to increase the rate of reverse intersystem crossing (k_{RISC}) according to the below equation;

$$kRISC \propto \exp\left(-\frac{\Delta E_{ST}}{k_B T}\right)$$

Other than that, a small ΔE_{ST} role is also significant for TADF emitters' lifetime. The performance of the emitters is also dependent on the PLQY, as it represents the efficiency of all non-radiative and radiative transition processes in the TADF molecule. The FWHM of the emission spectrum is substantial for the colour emission meanwhile, the stability of the molecular structure of TADF emitters is vital for its lifetime aside from the small ΔE_{ST}.

2.3 Molecular Design and Conformation

The molecular design and conformational have always been vital information for breakthroughs in studies. A report has been saying that the changes in conformational during excited state play the main role that reduces ΔE_{ST} and thus enhance the properties [6]. Based on the reports, they came out with two novel molecular designs which are twin D−A type (dimer) molecules and donor−acceptor (D−A) type (monomer) that were pre-twisted on their geometrical conformations as shown in Figure 4 and the results proved that the conformational change affected the ΔE_{ST}, where the monomers was proven to better candidate rather than dimers due to the steric effect of the two branches of the dimer [6]. The steric effect caused the dimer's conformation to be much more restricted and thus acting as a limiting factor for higher twisted torsional angle twisting to occur.

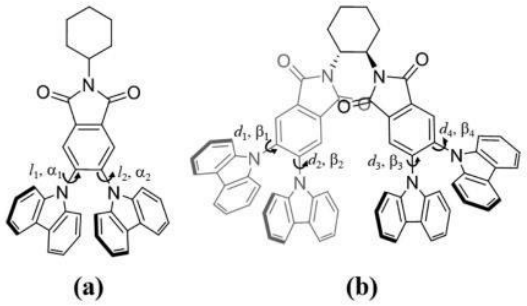

Figure 2.4. Molecular structure of (a) Monomer and (b) Dimer [6]

In this project, ground state ACRXTN molecular is studied by using the quantum molecular dynamics simulations. Because the molecule is bathed by thermal energy, the torsional angle of donor and acceptor should be different from calculation obtained from quantum molecular calculation such as Gaussian which performed the calculation at 0 K. As the slight changes in the conformational of the molecule can results differently, perhaps a breakthrough, or if not, a discovery will be obtained from the project. Other than that, the dihedral angle between the acceptor and donor atoms plays a major part in conformational geometry. Referring to a report in 2017 regarding the molecule design strategy of TADF emitters, the approaches used were increasing the torsional angle between the donor and acceptor through a linker and intensifying the donor/acceptor strength to decrease the ΔE_{ST} [8]. The ΔE_{ST} is generated as the minimalization of HOMO-LUMO spatial overlap to achieve higher efficiency.

Due to the requirement to have a big molecular size and for the fast and accurate screening of compounds, Density Functional Theory (DFT) is so far the most utilized computational tools [9]. Besides, conformational is one of the fundamentals in chemistry that affects the physical properties of the molecule significantly. For instance, the usage of a phenothiazine donor in 3,7-PTZ-DBTO2 in a report that it can adopt more than one stable conformer, with both the H-intra and H-extra folded conformers of the phenothiazine are possible. Remarkably, for H-intra conformational isomers, there is negligible overlap between HOMO and LUMO which is producing small ΔE_{ST} compared to H-extra [10].

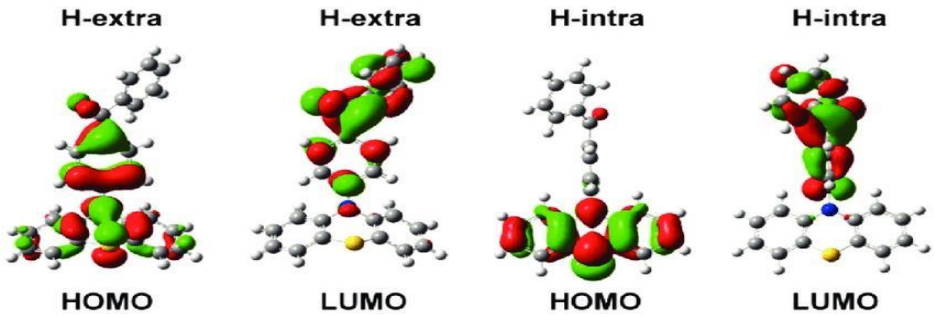

Figure 2.5. The computed HOMO and LUMO spatial distributions of PTZ-DBTO2-based H-extra and H-intra conformational isomers [10].

This permits the formation of perpendicular quasi-equatorial (eq) and parallel quasi-axial (ax) conformers. In recent years, dos Santos *et al*. mentioned that the excitation energy and environment polarity can control the molecular structure of the two D–A–D molecules, 2,7bis(phenothiazin-10-yl)-9,9-dimethylthioxanthene-S,S-dioxide(DPT-TXO2) and 2,7-bis(1 methylphenothiazin-10-yl)-9,9-dimethylthioxanthene-S,S-dioxide(DMePTTXO2) as shown in Figure 6 [12].

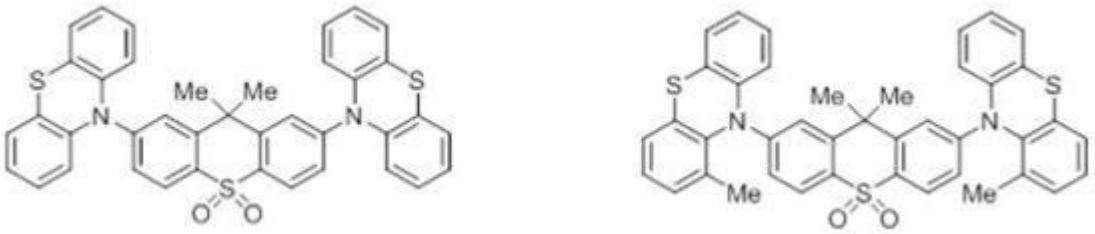

a) b)

Figure 2.6. Chemical structures of a) DPT-TXO2 and (b) DMePT-TXO2.[12]

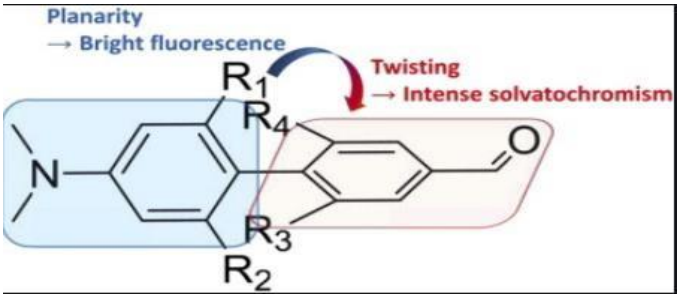

Figure 2.7. The design of donor-acceptor geometry for tuning excited-state polarization: fluorescence solvatochromism of push-pull biphenyls with various torsional restrictions on their aryl-aryl bonds [13].

The slightest change can give a large impact on the conformations, then exhibits varied TADF performance. In TADF, the localization of HOMO -LUMO at the D and A via C-N bridge at a certain angle (~60^o-80^o) is crucial for high PL quantum yield [14,15]. The torsional force that occurs between the donor unit and acceptor unit of the molecule is inhomogenous widened from the equilibrium geometry due to the intermolecular interaction and thermal fluctuation [15]. It can significantly increase the transition dipole moment (TDM) and spin-orbit couplings (SOCs) in the meantime controlling the ΔE_{ST} to retain small enough [15]. Despite the substantial unravelling of molecular conformation in a liquid state, there seems to be a minuscule number of reports available to date in solid-state. There is a need to quantify the distribution of the molecular conformations in solid to analyze such information to the observed physical properties. Thus, in this project, we want to quantify the distribution of the TADF molecular conformation in a solid-state and liquid state through molecular dynamics simulation.

2.4 Quantum Molecular Dynamic Simulations

Density functional theory (DFT) is a computational quantum mechanical modelling method to investigate the electronic structure of many-electrons. It can be used to determine the ground state and excited state geometry, the prediction of basic optical properties, and the importance of vibrionic coupling. The molecular design has been relying on the calculation of the excitation energies using time-dependent density functional theory (TD-DFT). Quantum molecular dynamics (QMD) simulations which are also known as *ab initio* performs a full quantum calculation of the electronic structure for every configuration of the atomic nuclei. In the simulations, the motions of the electrons are treated quantum mechanically using the Schrodinger equation to resolve the complicated equation due to many interacting electrons

and nuclei. Quantum methods are used to compute the forces while the classical atoms move according to Newton's equations in response to the interaction with other electrons and other forces. Molecular dynamics (MD) simulation is a computer simulation technique that computes the time evolution of an interacting particles system involving the generation of atomic trajectories of a system using numerical integration of Newton's equation of motion for a specific interatomic potential defined by an initial condition and boundary condition.

For QMD simulation, it has higher accuracy than the classical molecular dynamics simulation, but it needs much higher numerical efforts which restricts the number of atoms and the simulation time. Meanwhile, for classical MD the advantage of it is that it works well for much simpler particles (e.g., noble gases) that interact via isotropic pair potential, but poorly for covalent atoms and metals. There is a few assumptions and limitations of the classical molecular dynamic simulations. The first being in classical mechanics, the atoms are treated as a point mass where at low temperature (around 0-10 K) molecular motion is not describe perfectly, even at room temperature the detailed motion of light atoms (e.g., hydrogen atoms) is not described precisely [16]. Despite the shortcoming, the MD simulations are fast and permitting large particle numbers.

Currently, there is a lack of QMD treatment of TADF molecules, despite the fact TADF molecules can exhibit disorders due to thermal agitation in solvent. The vibronic coupling of the excited state is the one of the key factors that result in dark states to become bright states. Recently a molecular dynamic simulation is carried out that are used to mimic the evaporation process of a TADF molecule in a host of Bis[2-(diphenylphosphino)phenyl] ether oxide (DPEPO) [25]. An energy gap of 15 meV is obtained for ground state energy for SBABZ4 with torsional angle between donor and acceptor moieties being 86^{o} but in the experiment where the gap is found to be 72meV corresponding to torsional angle in the range of 70^{o} -75^{o}. Molecular dynamics involving 1000 molecules are simulated to calculate the disorder nature of SBABz4:DPEPO films at 1: 9 ratio. The probability density of the dihedral angle obtained in

MD also indicates two local maxima as shown in Figure 8(b) nearer to the experimental value (yellow values) [25]

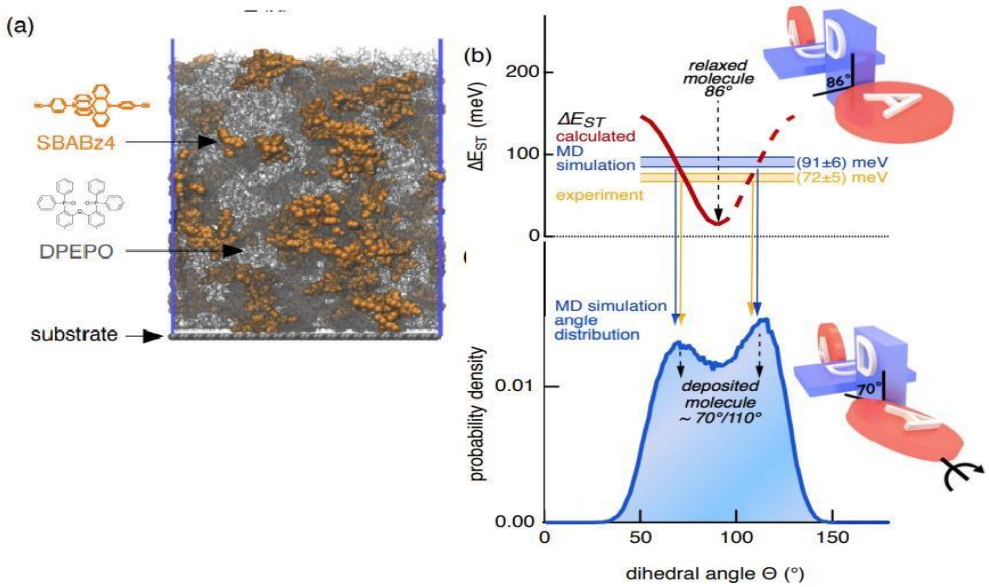

Figure 2.8. **(a)** MD simulation mimicking the evaporation process for a film of 10mol% of SBABz4 (orange space-filling models) in DPEPO (grey sticklike models) **(b)** TD-DFT calculations are performed to extract a mean ΔEST and the distribution of torsional angle Θ [25].

An example of the applications of both MD and QMD is the simulations are used to determine the organic molecules' surface wettability where the MD and QMD simulations are used on investigating the interactions between solid surfaces and droplets [17,24]. It is a useful method for understanding conformational dynamics and interactions in wetting. Comparison between theoretical and experimental results for the contact angle was done to prove the validity of both simulations [17,24]. In the experiment, the organic molecules such as oligomers and solvents are used as model polymers while the solid surface used as Al_2O_3 (0001) surface as shown in Figure 9 [17]. The snapshots of the wetting process and interfacial properties using QMD is as shown in Figure 10.

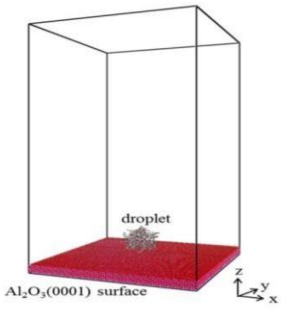

Figure 2.9. The initial construction for MD simulation of wetting the Al_2O_3 (0001) surface [17].

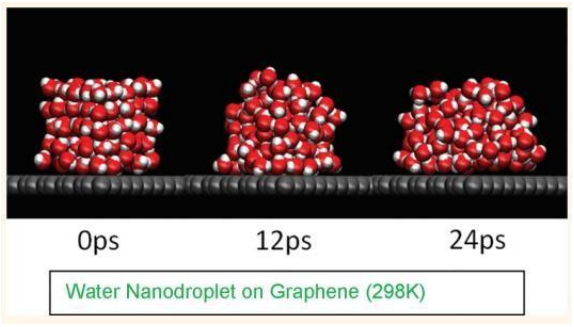

Figure 2.10. The wetting process of water nanodroplet on graphene sheet at 298K during the time evolution (in unit ps) by using Born-Oppenheim Quantum Molecular Dynamics simulation [24].

Recently, there is a report regarding the application of massive molecular dynamics simulation to strategize a model for vaccine development for the recent ongoing pandemic SARS-CoV-2 coronavirus. Molecular simulation is used to reveal the mechanistic intricacies of the virus at the atomic level. With the computational tool's assistance, the findings are vital for breakthroughs for a promising vaccine [18].

CHAPTER 3: RESEARCH METHODOLOGY

3.1 Methodology

The isolated structures are initially optimized at AM1 level using GAUSSIAN09. The optimization of all molecular geometries relied on density functional computations that are performed in Terachem 1.9[20] using the optimally tuned range-separated [21] LC-ωPBE functional at cc-pVDZ basis level under polarizable continuum model (PCM) with toluene as a solvent [22] or in solid matrix Zeonex. Using a 64 GB RAM GPU server, the computations were performed to support eight Tesla K10 graphic. Apart from the 6-31g basis set, the optimized geometries are then subjected to quantum molecular dynamics (QMD) simulations using the same functional theory [23]. With an equilibrium temperature of 500, 400K, and 300K, the initial temperature is set at 600K using Langevin as a thermostat. Langevin is chosen to simulate the effect of jostling of solvents or without it in a solid matrix. The QMD simulations are carried out with 1 femtosecond (fs) time step with 100000 steps. The solvent radius is set to be 3.48 Å and a dielectric constant of 2.38, typical values for toluene. Suitable molecules from ground state QMD are sampled to perform the first excited state QMD using time-dependent LC-ωPBE at the same basis level. Implementation of the time-reversible integrator with dissipation is also done. The simulations are also done using Machine Learning accelerated QMD Simulation using TORCHANI neural network. Calculation of dihedral angle using Python with predetermined the labelling of atoms by using GaussView. Comparison with classical molecular dynamic simulation (MD) carried out accelerated using machine learning codes.

3.2 Materials

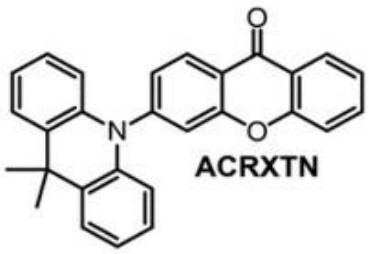

Figure 3.1. The molecular shape of TADF molecule, 3-(9,9-dimethylacridin-10(9H)-yl)-9H-xanthen-9-one (ACRXTN) in the host, Zeonex.

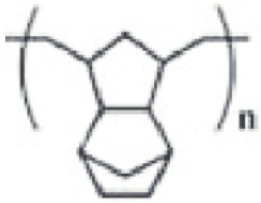

Figure 3.2 Host Molecular structure (ZEONEX)

3.3 Programming (Python)

Basic skills of python programming are needed for analysing the data. A python program is written to extract data from the simulation. Python is used to do large data analytics from the output from the gigabytes of data from the simulation as the raw data for each simulation is approximately 1 Gigabyte. The main objective for using the Python program is to extract the data for torsional angles between the donor and acceptor unit given varied different temperatures for both the solid and solvent host. Based on the simulation, coordinates for each atom are known which will lead us to compute the torsional angle. By using vectors which are the angles between planes formed by each atom we can determine the torsional angle which is usually calculated using the orthogonalized Cartesian coordinates.

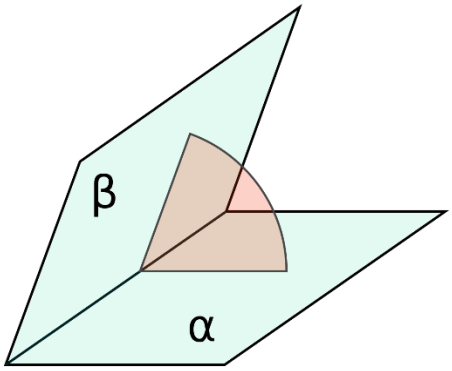

Figure 3.3. The dihedral angle is shown between two plane α and plane β.

The general equations that are used to calculate the dihedral angle are below;

Ax + By + Cz + D = 0 and its normal vector is represented by $\vec{n}$, then

$\vec{n}$ = (A, B, C)

Assume that the equations of two planes are given as;

$A_1 + B_1 + C_1 + D_1 = 0$ and $A_2 + B_2 + C_2 + D_2 = 0$

Then normal vector to those planes are ,

$\overrightarrow{n1}$ = (A_1, B_1, C_1) and $\overrightarrow{n2}$ = (A_2, B_2, C_2)

Let θ be the angle between the planes, then the formula would be given as below:

$\cos\theta = \frac{\overrightarrow{n_1} \cdot \overrightarrow{n_2}}{\overrightarrow{n_1}\overrightarrow{n_2}}$ or can be written as

$$\cos\theta = \frac{|A_1A_2 + B_1B_2 + C_1C_2|}{\sqrt{A_1^2+B_1^2+C_1^2}\sqrt{A_2^2B_2^2C_2^2}}$$

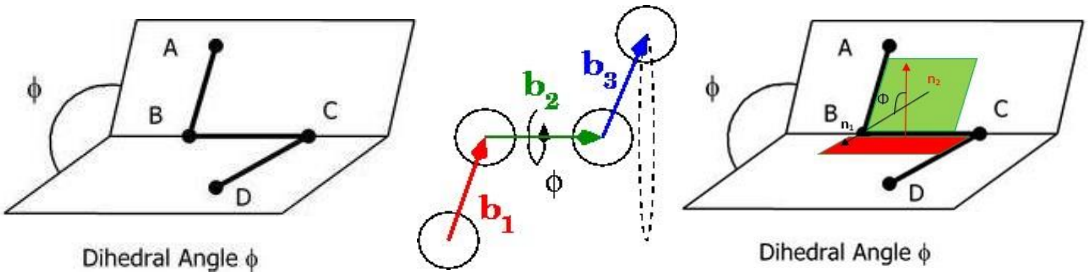

a) **b)** **c)**

Figure 3.4. a) The four points on the planes and the angle between the two planes **b)** The four points and their vectors obtained from vector subtraction **c)** The dihedral angle between the four points in two planes.

For given four Cartesian coordinates;

A = (A_x, A_y, A_z)

B = (B_x, B_y, B_z)

C = (C_x, C_y, C_z)

D = (D_x, D_y, D_z)

By using the vector subtraction to obtain the vectors;

$\vec{b}_1$ = B – A

$\vec{b}_2$ = C – B

$\vec{b}_3$ = D – C

By using $\langle b \rangle$ to denote $\frac{b}{||b||}$ the unit vector in the direction of the vector v.

$\overrightarrow{n_1} = \langle b_1 \times b_2 \rangle$ and $\overrightarrow{n_2} = \langle b_2 \times b_3 \rangle$

Let θ be the angle between the planes, then the formula would be given as below;

$\cos\theta = \frac{\overrightarrow{n_1} . \overrightarrow{n_2}}{\overrightarrow{n_1}\,\overrightarrow{n_2}}$ or which is as shown in the Figure 12 (c)

For ACRXTN molecule, the location of the four points A, B, C, D are defined as below;

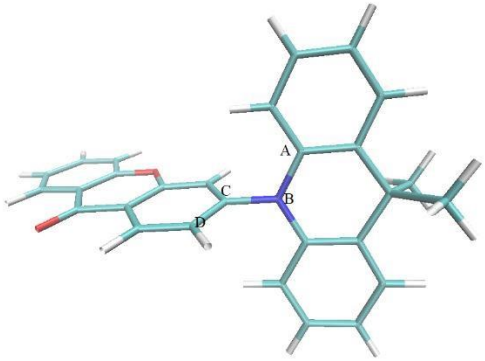

Figure 3.5. The four points A, B, C, D on two planes in the molecular structure of ACRXTN.

PyTorch is an open-source machine learning library based on the Torch library that is mainly used for computer vision and natural language processing and it is the most used and popular among researchers due to its ease to use and flexibility [26]. In QMD simulation accelerated by machine learning, TorchANI is the ANI neural network potentials that is being implemented on PyTorch with the intended use to be light weight, cross platform, user friendly and easy for reading and modifying [27].

CHAPTER 4: RESULTS AND DISCUSSIONS

4.1 Introduction

TADF molecule was simulated using two approaches: (1) Full Quantum Molecular Dynamics simulations in explicit host and (2) Quantum Molecular Dynamics with explicit host accelerated with machine learning. In full QMD, because of the highly computational demanding calculation, it contains only 1 TADF molecule and 4 molecules for Zeonex and for QMD accelerated machine learning, it has 1 TADF molecule and 13 molecules of Zeonex**.** In Full QMD, we have 396 atoms meanwhile accelerated QMD consists of 1170 atoms. Both approaches were simulated at different temperatures. The first approach was simulated at temperatures of 300K, 400K,500K and 600K meanwhile the second approach was simulated at temperatures of 150 K, 200 K, 250 K, 300 K, 350 K, 400 K, 450 K, 500 K and 600 K. The former approach is highly computational demanding and hence only a small range of temperature and Zeonex molecules are simulated. Both approaches were run in the DICC cloud computing, and the data are analysed using Python Programming Language (Anaconda/SPYDER).

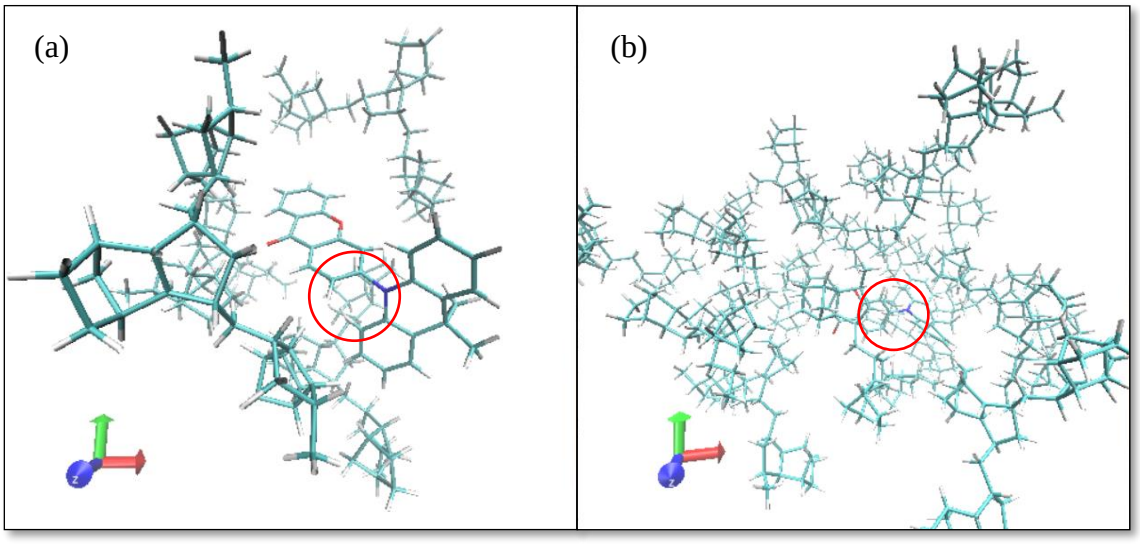

Figure 4.1. TADF molecules in the host simulated for **a)** full QMD simulation, and **b)** QMD with accelerated machine learning using Virtual Molecular Dynamics (VMD). The red circles show the dihedral angle of TADF molecule inside the host.

Referring to **Figure 4.1**, in both system the TADF molecule that has been embedded in the host Zeonex but with different precise positioning of the Zeonex with respect to the TADF

molecules. A larger system is used in QMD accelerated by machine learning than in the full QMD due to time and computational intensiveness of full QMD. By using VMD, the conformational changes can be studied and observed in much more details.

4.2 Results

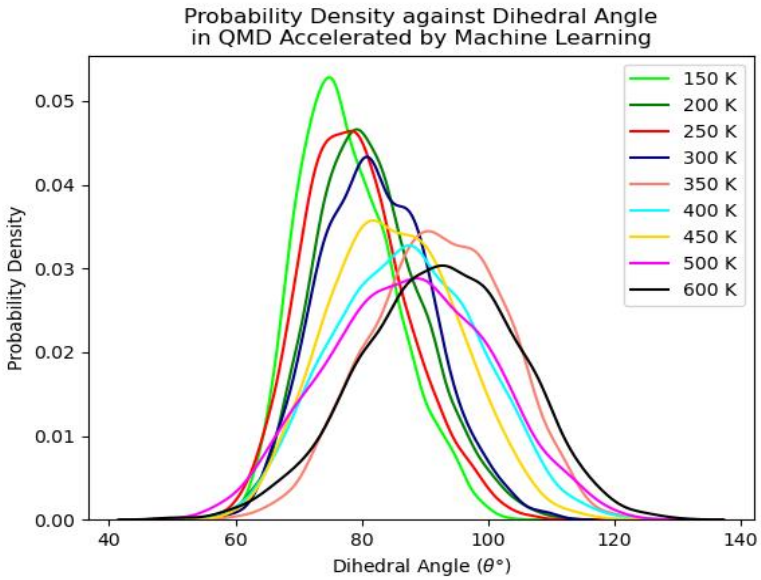

Figure 4.2 The probability density of the dihedral angles between donor and acceptor of a TADF molecule at different temperatures (K) simulated using QMD accelerated by machine learning. The data points that are used to construct each curve for each temperature used are approximately 4500 data points for each point with incremental angle of ± 3º.

Figure 4.2 shows the probability density of the dihedral angles between donor and acceptor of a TADF molecule at different temperatures simulated using machine leaning QMD. As seen in **Figure 4.2**, as the probability spread increases as the temperature increases; so as the peak of the distribution (mode) shifts to a larger angle. The probability density at 150 K has the highest peak compared to other temperatures as the 'gaussian' spread is the lowest. At 150 K, the TADF molecule gains less kinetic energy from the surrounding compared at a higher temperature. Optimizing the molecular structure of a single TADF using full QMD and representing the host as a continuous medium instead of individual molecules, the dihedral angle obtained for a single molecule calculated at 0K is 90.68º. This value is very different from the mode of the dihedral angle even at 150 K. Considering the trend, the machine learning accelerated QMD, at even lower temperature (~ i.e., 20 K), would be lower than 75º. In host, the dihedral rotation of TADF molecule is restricted compared in free space or continuous medium. By explicating the host molecules, since no electrons of the same spin can occupy at

the space, this generated restricted dihedral rotation in the presence of host. As the temperature increases, more energy is available for the TADF molecule to overcome such restriction and the mode is more representative of the TADF equilibrium position.

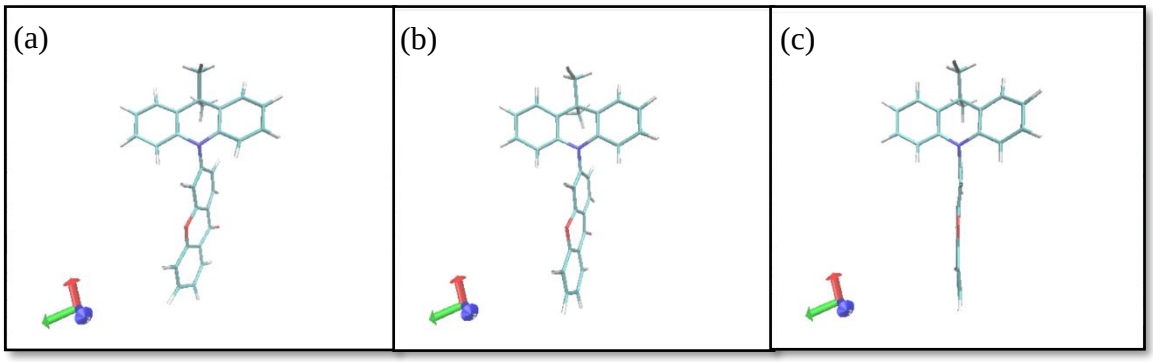

Figure 4.3 The conformation of TADF molecule for 150 K at (a) 60º (b) Peak (c) 100º using VMD.

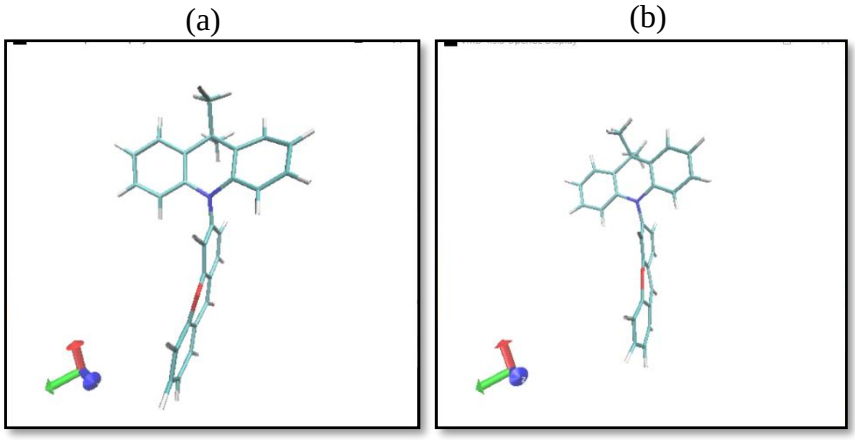

Figure 4.4 The conformation of TADF molecule at the peak for (a) 300 K and (b) 400 K using VMD.

Figure 4.3 and **Figure 4.4,** show the representative of TADF conformation extracted out from the host illustrating the changes of TADF molecule. In **Figure 4.3**, the differences of the conformation for different dihedral angles are shown for TADF molecule at 150 K for three different dihedral angles which are 60º, 75º (peak) and 100º. The distortion of dihedral angle even at same temperature occurs due to the dihedral vibrational around the donor and acceptor of the TADF molecule itself as the collisions of atoms happen. **Figure 4.4 (a)**, and **(b)**, show the representative TADF conformation mode at 300K and 400K.

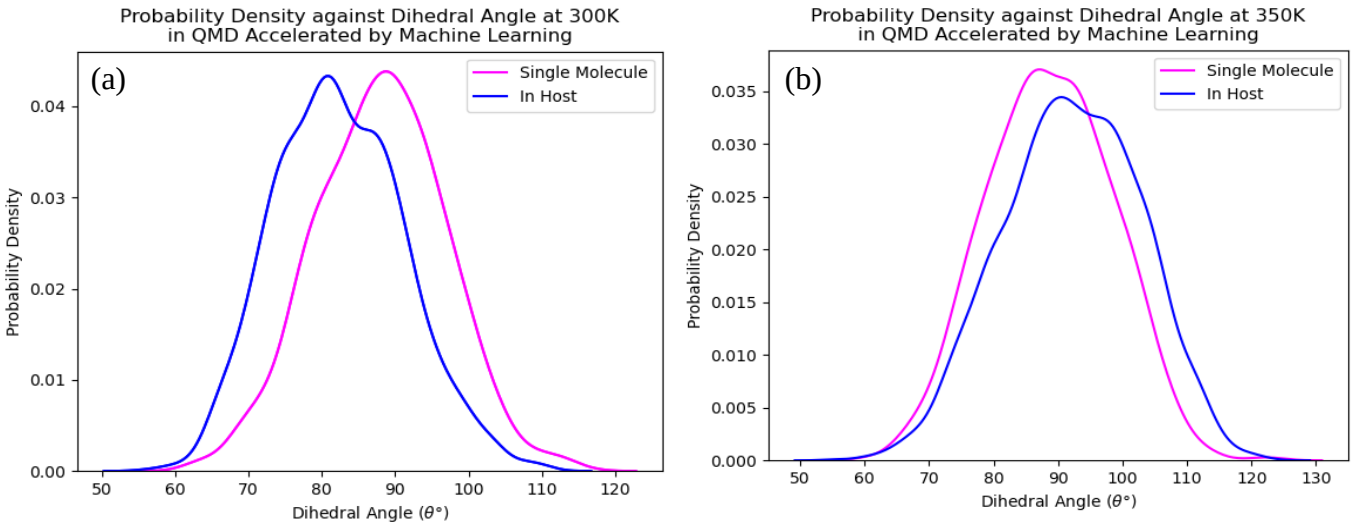

Figure 4.5 Comparison of the probability density of the dihedral angles in single molecule and embedded in host at (a) 300K and (b) 350K using the QMD accelerated with machine learning.

Figure 4.5 illustrates the comparison of the probability density of the dihedral angles of the TADF molecule using QMD accelerated by machine learning at 300K and 350K. The peaks for the probability density at 300K for both single molecule and embedded in host are almost similar where the mode for single molecule is 89º and 81º respectively. At 350K, the mode for TADF molecule in single molecule is 93º and in host is 90º respectively. In **Figure 4.6,** the median points for dihedral angle of TADF molecule in a single molecule have a much larger angle than TADF molecule embedded in host. When the TADF molecule is embedded in a host, the larger system the more molecules imposing restriction on the conformational of the TADF molecule.

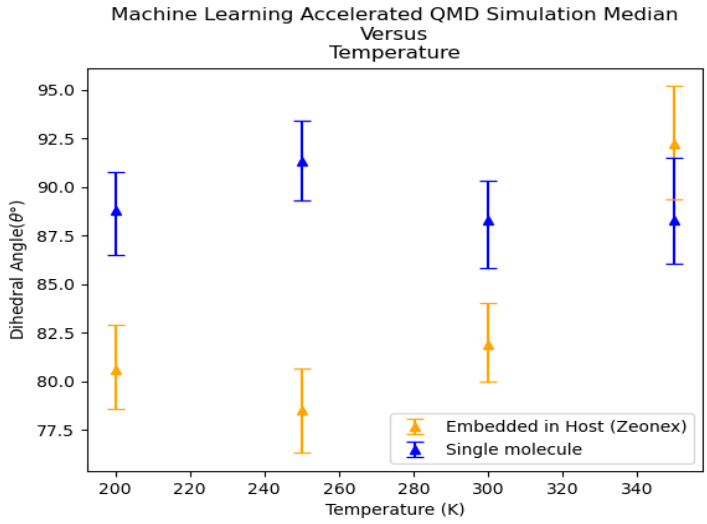

Figure 4.6 The median with its standard deviation in single molecule and embedded in host with different temperature using the QMD accelerated by machine learning.

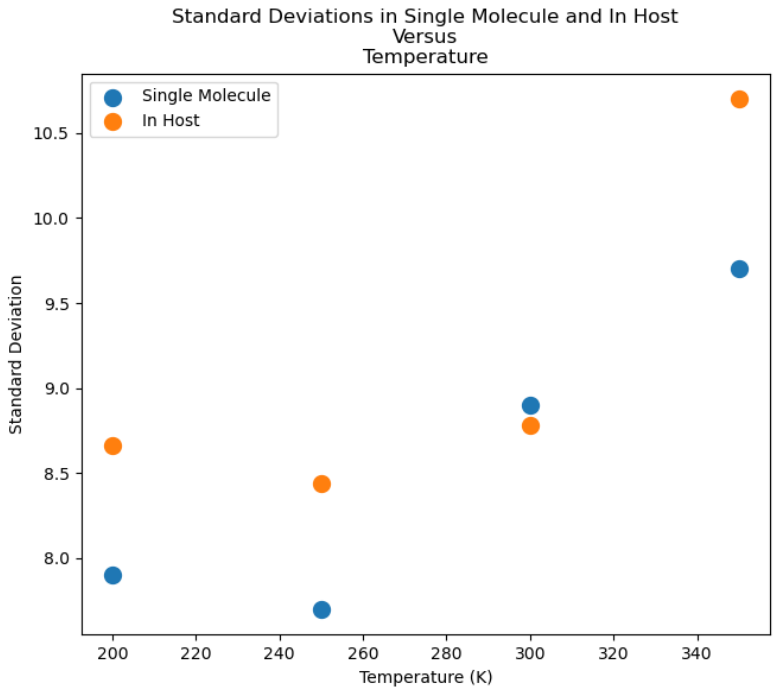

Figure 4.7 The standard deviation in single molecule in vacuum and single molecule embedded in host with different temperature using the QMD accelerated by machine learning.

Temperature (K)	**Standard Deviation**	
	Single Molecule (θ^o)	In Zeonex as a Host (θ^o)
200	7.88	8.66
250	7.72	8.44
300	8.87	8.78
350	9.72	10.7

Table 1: The standard deviation of the dihedral angle of the TADF molecule as single molecule in vacuum and single molecule embedded in host with different temperature using the QMD accelerated by machine learning.

Figure 4.7 shows the graphic illustration of the data in **Table 1**. Generally, it is discerned that the standard deviation of the dihedral angle of TADF molecule in a single molecule in vacuum is lower than when it is embedded in host (Zeonex). The TADF molecule embedded in host tends to spread more in the probability density function rather than as a single molecule in vaccuum.

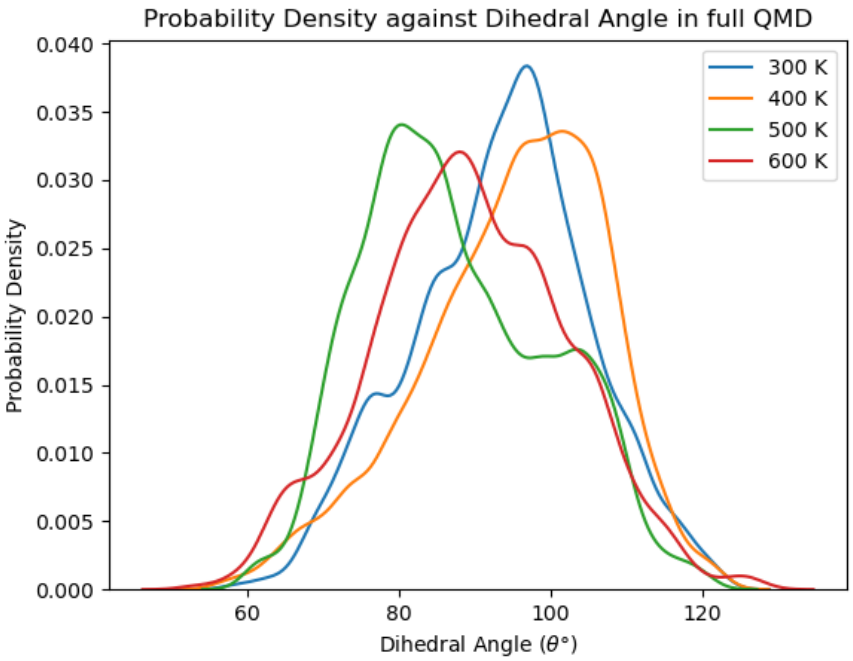

Figure 4.8 The probability density of the dihedral angles between donor and acceptor of a TADF molecule at different temperatures (K) in full QMD. The data points used are approximately in 10000 data points.

In **Figure 4.8,** the graphs illustrate the probability density of dihedral angle between the donor and acceptor at different temperatures in full QMD. The pattern of the graph in **Figure 4.8** shows increment of the dihedral angle between the donor and acceptor as the temperature incraesed, while the maximum probability density (height of the mode) is decreasing. However, trends of the shift of the mode cannot be discerned clearly as in **Figure 4.8** compared with **Figure 4.2**.

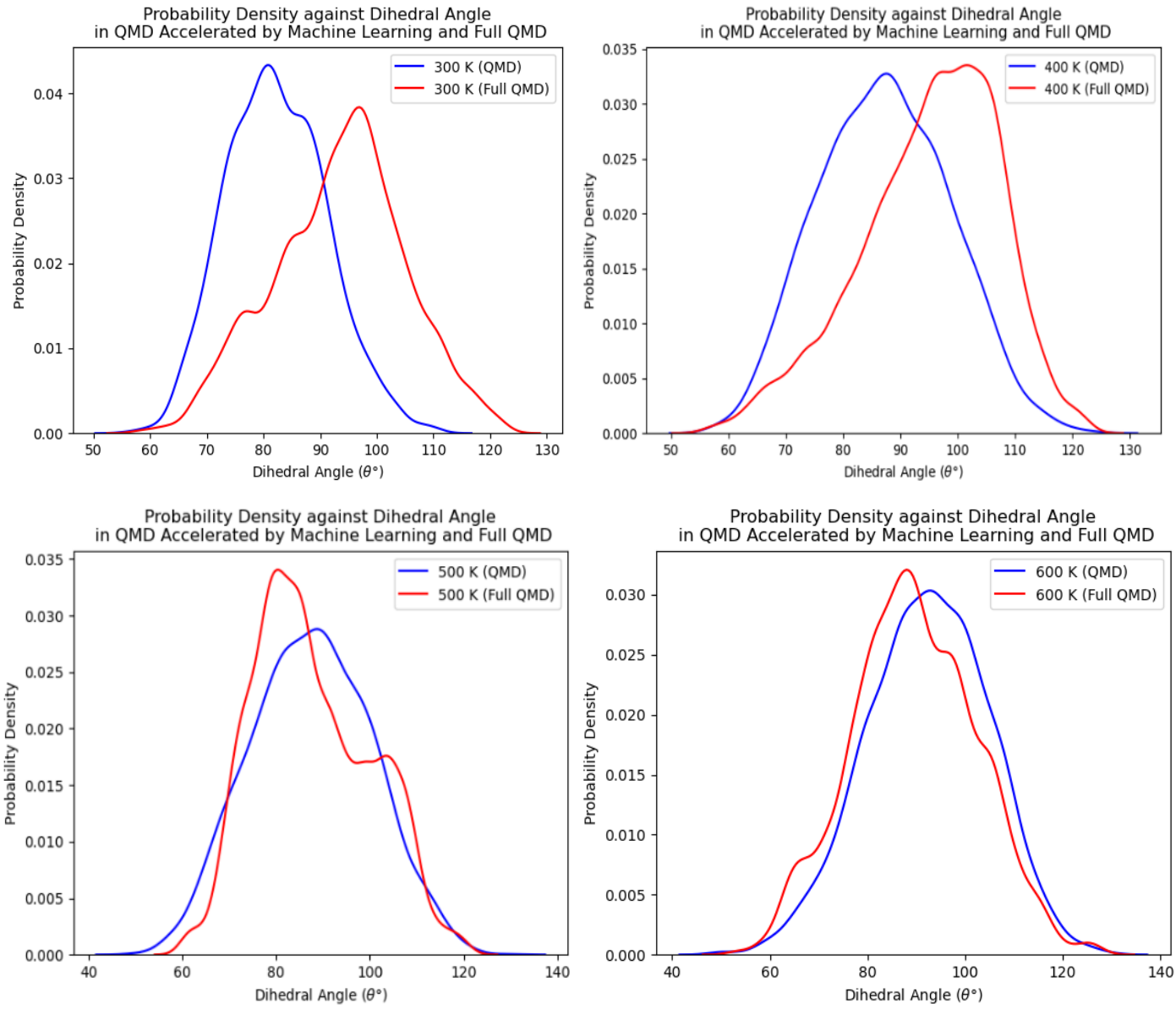

Figure 4.9 Comparison of probability density of the dihedral angles between donor and acceptor of a TADF molecule for full QMD simulations and machine learning accelerated QMD simulations against different temperatures (a) 300 K (b) 400 K (c) 500 K and (d) 600 K.

In **Figure 4.9**, the probability density for QMD with machine learning accelerated is smoother as compared to full QMD. The temperature for both QMD accelerated machine learning and full QMD at 600 K have a near similar probability density as to compare with the temperatures and to lesser extend for 500K but not at 300 K and 400K. The mode for 600K and 500K are near to each other between the two methods (90 º and 99 º at 600K and 79 º and 89 º at 500K for full QMD and machine learning accelerated QMD, respectively. We hypothesize that because in full QMD there is far less Zeonex is simulated which restrict the dihedral vibration

of the TADF molecule compared with the machine learning accelerated QMD, the TADF molecule in the machine learning accelerated QMD can only move more freely at higher temperature (ie 600K) due to expansion and higher kinetic energy and hence approaches the results similar to full QMD. This has an important implication that simulation a larger system would be more representative of a real system.

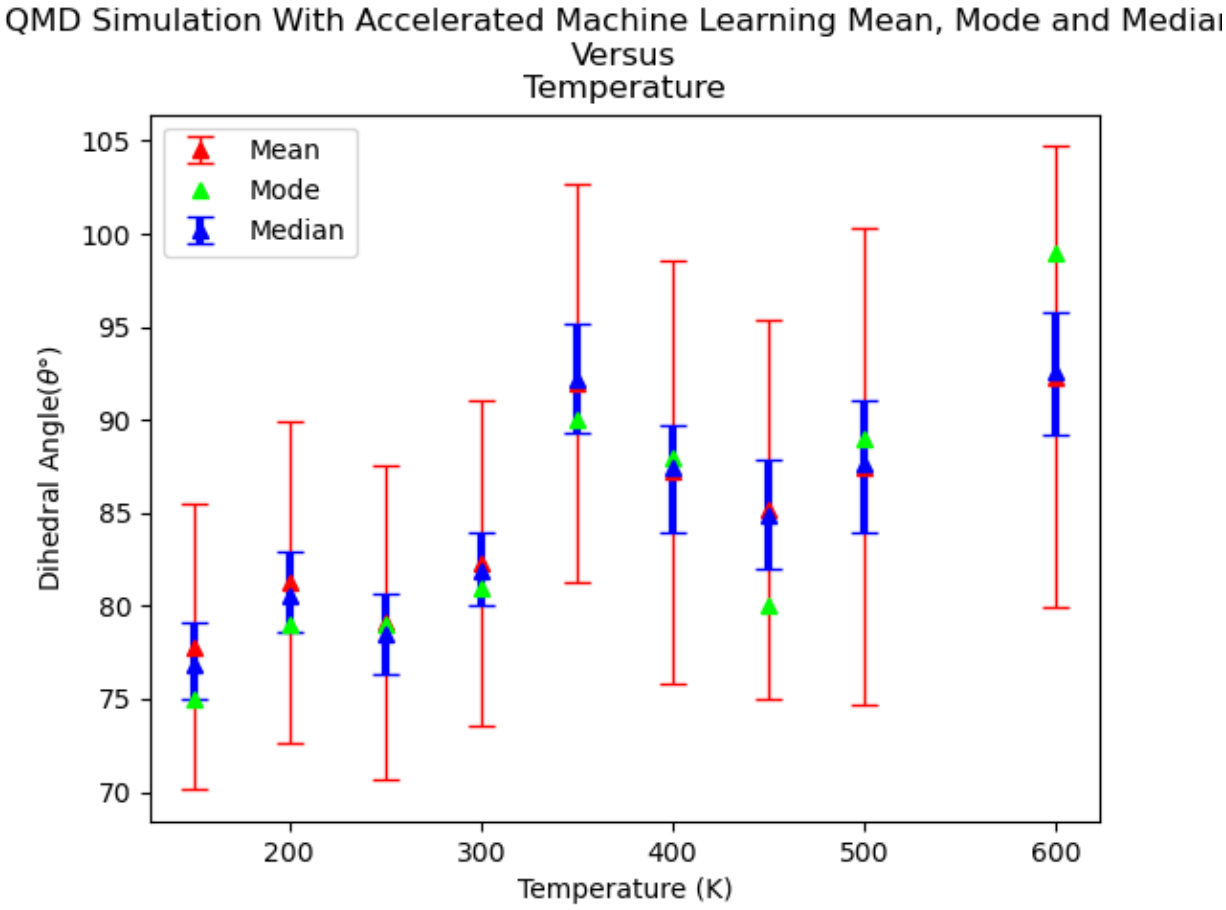

Figure 4.10 The mean along with the standard deviation as the error bar, median +/10% with 60%, 40% error bar and mode values of the dihedral angles along with their standard deviation for QMDs with accelerated machine learning against different temperatures.

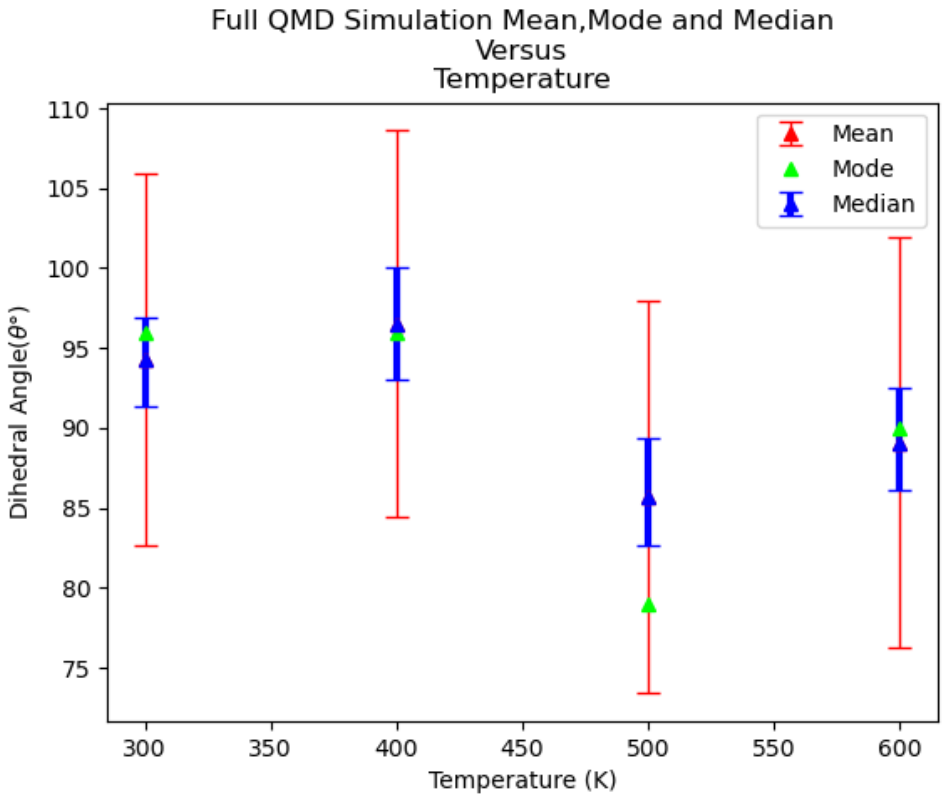

Figure 4.11 The mean along with the standard deviation as the error bar, median +/10%, and mode values of the dihedral angles for full QMDs against different temperatures.

Referring to both figures, the trends show inconsistency, where the mean value from 150 K to 350 K shows a generally increasing trend which then starts to decline to 500 K and, increase again until 600 K for Figure 1. In **Figure 4.10**, the mean value is the highest, which is 92.3 º, when the temperature is at 600 K and the lowest is at 150 K with angle of 77.8 **º**. Based on **Figure 4.11**, the mean values for the first half are showing a slight increase in angle, then the value starts to drop from 400 K until it reaches 500 K then increases slightly at 600 K. The highest and lowest mean values are at 400 K and 500 K where the dihedral angles are 95 º and 87.6 **º** respectively. From both **Figure 4.10** and **Figure 4.11,** we can observe that the temperature does have a slight effect on the dihedral angle of TADF molecule. As the temperature increases, the TADF molecule gained more kinetic energy to alter its conformation. The mean, median and mode of the dihedral angles deduced from **Figure 4.10** and **Figure 4.11** are similar with each other.

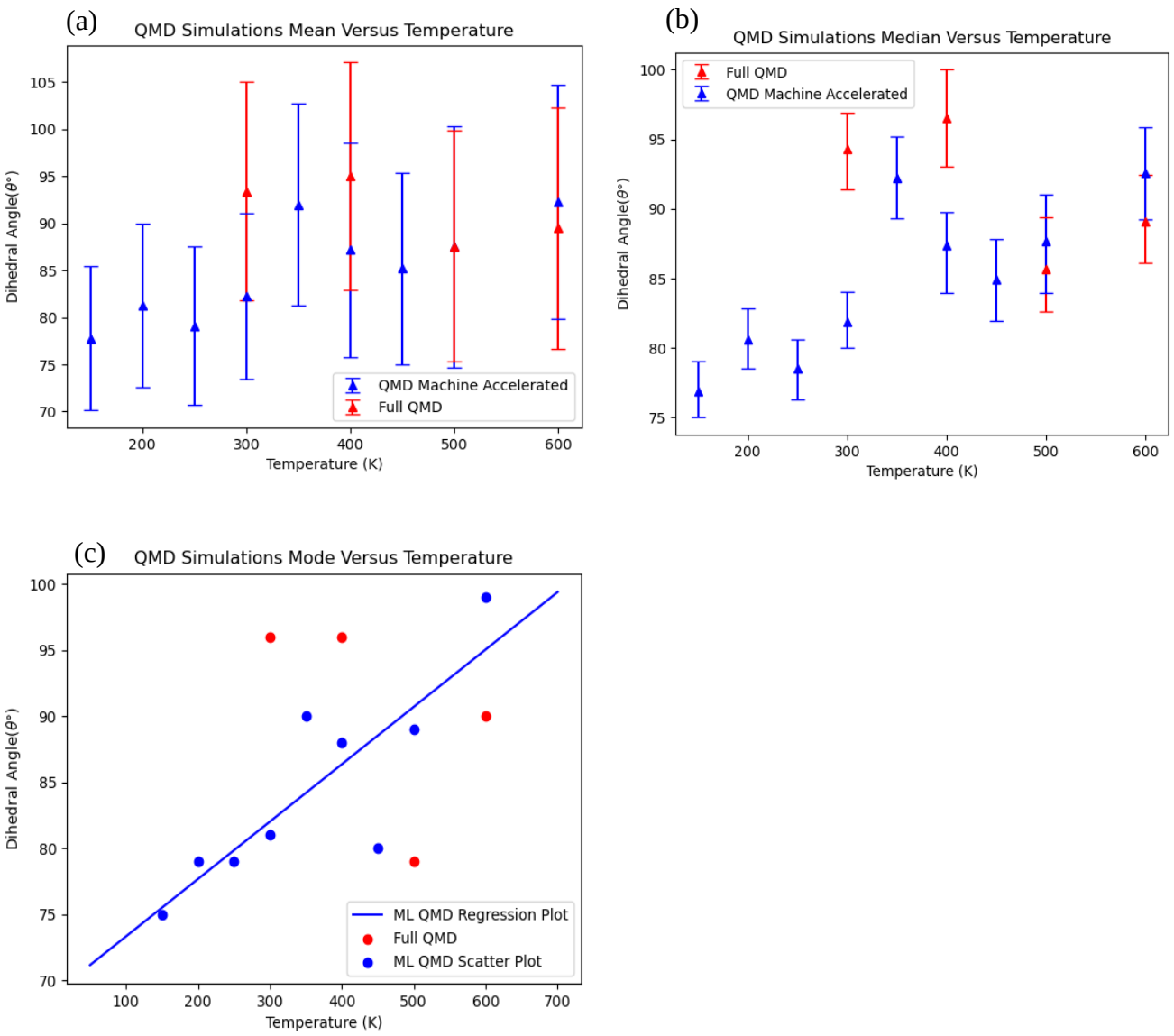

Figure 4.12 Comparison of the (a) mean with standard deviation as the error bar, (b) median +/10%, and (c) mode values between full QMD simulations and machine learning accelerated QMD simulations against different temperatures.

Comparison of mean values for both approaches is done as in **Figure 4.12**. The mean values for both approaches at 300 K, 400 K, 500 K and 600 K are overlapping. These overlapping shows that both simulations approaches may generate almost similar results.

CHAPTER 5: CONCLUSIONS

5.1 Conclusion

In machine learning accelerated QMD, the dihedral angle shifts to larger angle as the temperature increased but this cannot be seen in full QMD. This is probably due to smaller system and time scale of simulation. For full QMD, the time scale used for simulation is not long enough, even for single molecule, it must be greater than 10,000 fs meanwhile the time scale of machine learning accelerated QMD is 500,000 fs. Machine learning accelerated QMD is superior in terms of speed and timescale of simulations, and ability to simulate the more complex system (i.e., More host molecules). The dihedral angle of TADF molecule embedded in a host tends to spread more than as a single molecule in a vacuum.

5.2 Suggestion for Further Work

Since the machine learning QMD suggested that dihedral angle of TADF molecule embedded in a host has a larger spread compared with a single molecule in host, experimental evidences need to be gathered to support this discovery. Further, temperature has an effect of the dihedral angle and experimental evidence to support that will be the future works. QMD simulations is a compelling process. Using QMD simulation to look within atoms and molecules, more theoretical guided experiments can be done due to its high credibility. In the meantime, as QMD simulation accelerated with machine learning is proven to be more superior to full QMD, machine learning accelerated QMD is possibly a great alternative method to conduct more virtual experiments.

REFLECTION

Final year project is indeed the most vital assignment for undergraduate student during our studies. It is also the most complex, strenuous, and full of challenges but the returns and benefits that I gain is worthy of the time and effort. Final year project is half a step into the reality especially in research field and it is a form of preparation for me before stepping into real life working world.

My project is about Quantum Molecular Dynamic Simulation in Thermally Activated Delayed Fluorescence. Initially, I was quite afraid to choose this project, because given the pre-requisite is that I need to learn how to use programming software for extracting the data and I realized that programming has never been my strong suit. Given limited choice and time, I tried to challenge myself give a shot at this project and learn more about programming. I believe that I will be able to grasp programming better if I keep practising at it because for me, no hard work will go to waste.

In these two semesters completing my project, I am very grateful for having a very kind, and dedicated supervisor, Assoc. Prof. Dr Woon Kai Lin who has always guide me with programming and let me understand the software better. A long the way I have learnt a lot of discoveries and exposed to me to how far science has gone until today. All the things that I have learnt is just the tip of an iceberg. Finally, my greatest gratitude to my supervisor for all his time and effort in giving me his helping hands.

REFERENCES

1. Uoyama, H.; Goushi, K.; Shizu, K.; Nomura, H.; Adachi, C. Highly efficient organic lightemitting diodes from delayed fluorescence. Nature 2012, 492, 234−238.

2. Pope, M.; Kallmann, H. P.; Magnante, P. Electroluminescence in Organic Crystals. J. Chem. Phys. 1963, 38, 2042−2043.

3. Perrin, F. Fluorescence of solutions. Ann. Phys. (Paris, Fr.) 1929, 10, 169−275.

4. Olivier Y., Sancho-Garcia J., Muccioli L., D'Avino G., & Beljonne D. (2018). Computational Design of Thermally Activated Delayed Fluorescence Materials: The Challenges Ahead. *The Journal of Physical Chemistry Letters*, *9*(20), 6149-6163. doi:10.1021/acs.jpclett.8b02327

5. Rajamalli P., Senthilkumar N., Huang P-Y., Ren-Wu C.-C., Lin H.-W., & Cheng C-H. (2017). New Molecular Design Concurrently Providing Superior Pure Blue, Thermally Activated Delayed Fluorescence and Optical Out-Coupling Efficiencies. *Journal of the American Chemical Society*, *139*(32), 10948–10951. https://doi.org/10.1021/jacs.7b03848

6. Zhang Wei, Song HW, Kong J, Kuang Z.R., Li M., Guo Q.J., Chen C.F., Xia A.D., "Importance of Conformational Change in Excited States for Efficient Thermally Activated Delayed Fluorescence", *Journal of Physical Chemistry* C,123,19322-19332,2019. https://doi.org/10.1021/acs.jpcc.9b03867

7. Yang Z., Mao Z., Xie Z., Zhang Y., Liu S., Zhao J., Xu J., Chi Z., & Aldred M. P. (2017). Recent advances in organic thermally activated delayed fluorescence materials. *Chemical Society Reviews*, *46*(3), 915–1016. https://doi.org/10.1039/c6cs00368k

8. Im Y., Kim M., Cho Y. J., Seo, J-A., Yook K. S., & Lee J. Y., (2017). Molecular Design Strategy of Organic Thermally Activated Delayed Fluorescence Emitters. *Chemistry of Materials*, *29*(5), 1946–1963. https://doi.org/10.1021/acs.chemmater.6b05324

9. Chen X.-K., Kim D., & Brédas J.-L. (2018). Thermally Activated Delayed Fluorescence (TADF) Path toward Efficient Electroluminescence in Purely Organic Materials: Molecular Level Insight. *Accounts of Chemical Research*, *51*(9), 2215–2224. https://doi.org/10.1021/acs.accounts.8b00174

10. Li C., Liang J., Liang B., Li, Z., Cheng Z., Yang G., & Wang Y. (2019). An Organic Emitter Displaying Dual Emissions and Efficient Delayed Fluorescence White OLEDs. *Advanced Optical Materials*, *7*(10), 1801667. https://doi.org/10.1002/adom.201801667

11. Penfold T. J., Dias F. B., & Monkman A. P. (2018). The theory of thermally activated delayed fluorescence for organic light emitting diodes. *Chemical Communications*, *54*(32), 3926–3935. https://doi.org/10.1039/c7cc09612g

12. dos Santos P. L., Ward J. S., Batsanov A. S., Bryce M. R., & Monkman A. P. (2017). Optical and Polarity Control of Donor–Acceptor Conformation and Their ChargeTransfer States in Thermally Activated Delayed-Fluorescence Molecules. *The Journal of Physical Chemistry C*, *121*(30), 16462–16469. https://doi.org/10.1021/acs.jpcc.7b03672

13. Sasaki, S., Niko, Y., Klymchenko, A. S., & Konishi, G.-. (2014). Design of donor–acceptor geometry for tuning excited-state polarization: fluorescence solvatochromism of push–pull biphenyls with various torsional restrictions on their aryl–aryl bonds. *Tetrahedron*, *70*(41), 7551–7559. https://doi.org/10.1016/j.tet.2014.08.002

14. Kwon-Hyeon Kim, Jang-Joo Kim, "Origin and Control of Orientation of Phosphorescent and TADF Dyes for High-Efficiency OLEDs", Advanced Materials, 2018 30, 1705600

15. Hu T., Han G., Tu Z., Duan R., & Yi Y. (2018). Origin of High Efficiencies for Thermally Activated Delayed Fluorescence Organic Light-Emitting Diodes: Atomistic Insight into Molecular Orientation and Torsional Disorder. *The Journal of Physical Chemistry C*, *122*(48), 27191–27197. https://doi.org/10.1021/acs.jpcc.8b08169

16. van Gunsteren, W. F., & Berendsen, H. J. C. (1990). Computer Simulation of Molecular Dynamics: Methodology, Applications, and Perspectives in Chemistry. *Angewandte Chemie International Edition in English*, *29*(9), 992–1023. https://doi.org/10.1002/anie.199009921

17. Suganuma, Y., Yamamoto, S., Kinjo, T., Mitsuoka, T., & Umemoto, K. (2017). Wettability of Al2O3 Surface by Organic Molecules: Insights from Molecular Dynamics Simulation. *The Journal of Physical Chemistry B*, *121*(42), 9929–9935. https://doi.org/10.1021/acs.jpcb.7b07062

18. Arantes P. R., Saha A., & Palermo G. (2020). Fighting COVID-19 Using Molecular Dynamics Simulations. *ACS Central Science*, *6*(10), 1654–1656. https://doi.org/10.1021/acscentsci.0c01236

19. Data P., & Takeda Y. (2019). Recent Advancements in and the Future of Organic Emitters: TADF- and RTP-Active Multifunctional Organic Materials. *Chemistry – An Asian Journal*, *14*(10), 1613–1636. https://doi.org/10.1002/asia.201801791

20. Ufimtsev I. S., & Martinez T. J. (2009). Quantum Chemistry on Graphical Processing Units. 3. Analytical Energy Gradients, Geometry Optimization, and First Principles Molecular Dynamics. *Journal of Chemical Theory and Computation*, *5*(10), 2619–2628. https://doi.org/10.1021/ct9003004

21. Sun H., Zhong C., & Brédas J.-L. (2015). Reliable Prediction with Tuned RangeSeparated Functionals of the Singlet–Triplet Gap in Organic Emitters for Thermally Activated Delayed Fluorescence. *Journal of Chemical Theory and Computation*, *11*(8), 3851–3858. https://doi.org/10.1021/acs.jctc.5b00431

22. Liu F., Luehr N., Kulik H. J., & Martínez T. J. (2015). Quantum Chemistry for Solvated Molecules on Graphical Processing Units Using Polarizable Continuum Models. *Journal of Chemical Theory and Computation*, *11*(7), 3131–3144. https://doi.org/10.1021/acs.jctc.5b00370

23. Woon K. L., Mustapa S. A. S., Mohd Jamel N. S., Lee V. S., Zakaria M. Z., & Ariffin, A. (2020b). Effect of Bulky Functional Groups on Donor and Acceptor Interactions and their Photoluminescence Properties. *ChemPhysChem*, *21*(22), 2620–2626. https://doi.org/10.1002/cphc.202000612

24. Li, H., & Zeng, X. C. (2012). Wetting and Interfacial Properties of Water Nanodroplets in Contact with Graphene and Monolayer Boron–Nitride Sheets. *ACS Nano*, *6*(3), 2401–2409. https://doi.org/10.1021/nn204661d

25. Sebastian Weissenseel, Nikita A. Drigo, Liudmila G. Kudriashova, Markus Schmid, Thomas Morgenstern, Kun-Han Lin, Antonio Prlj, Clémence Corminboeuf, Andreas Sperlich*, Wolfgang Brütting, Mohammad Khaja Nazeeruddin*, and Vladimir Dyakonov(*2019*). An Organic Emitter Displaying Dual Emissions and Efficient Delayed Fluorescence White OLEDs. . *Phys. Chem. C, 123, 45, 27778–27784*. https://doi.org/10.1021/acs.jpcc.9b08269

26. Yegulalp, S. (2017, January 19). Facebook brings GPU-powered machine learning to Python. Retrieved April 25, 2021, from https://www.infoworld.com/article/3159120/facebook-brings-gpu-powered-machine-learning-to-python.html

27. Gao X., Ramezanghorbani,F., Isayev, O., Smith J. S., & Roitberg A. E. (2020). TorchANI: A Free and Open Source PyTorch-Based Deep Learning Implementation of the ANI Neural Network Potentials. *Journal of Chemical Information and Modeling*, *60*(7), 3408–3415. https://doi.org/10.1021/acs.jcim.0c00451

APPENDICES

APPENDIX A

Machine Learning QMD Simulation

```
from ase import Atoms
from ase.optimize import BFGS
import torchani
from ase import units
from ase.md.langevin import Langevin
def atomicmass(a):
    if a=='H':
        a=1
    if a=='C':
        a=6
    if a=='N':
        a=7
    if a=='O':
        a=8
    if a=='S':
        a=16
    return a
mymolecule=[]
myposition=[]
myatom=[]
fp=open(r'C:\Users\Nurul\Desktop\FYP\Data\TADF in Zeonex\ACRXTN-2.xyz', 'r')
# Path Of The File
for i,line in enumerate(fp):
    line1=line.strip('\n')
    line1=line.split()
```

```
if i>1:
        mymolecule.append(atomicmass(line1[0]))
        myatom.append(line1[0])
        atomposition=(float(line1[1]),float(line1[2]),float(line1[3]))
        myposition.append(atomposition)
    if i==0:
        line1=line.strip('\n')
        line1=int(line1)
        noatom=int(line1)
molecule = Atoms(numbers=mymolecule,positions=myposition)
print(myatom)
calculator = torchani.models.ANI2x().ase()
molecule.set_calculator(calculator)
print("Begin minimizing...")
opt = BFGS(molecule)
opt.run(fmax=0.0001)
print()
Z=molecule.get_positions()
path=r'C:\Users\Nurul\Desktop\FYP\Data\TADF in Zeonex\ACRXTN-2.txt'
#Path Of The File
with open(path, "r") as ff: # or "rb"
    file_data = ff.read()
# And then:
raw = open(path, "w")
def storexyz(noatom,Z,m):
    myposition2=[]
    myposition2.append(str(noatom))
    with open(path, "a") as f:
    f.write(str(noatom)+"\n")
```

```
    with open(path, "a") as f:
        f.write(m)
    myposition2.append(" ")
    for i,line in enumerate(Z):
        a,b,c=line[0],line[1],line[2]
        a=str(a)
        b=str(b)
        c=str(c)
        atomposition=str(myatom[i])+"   "+a+"   "+b+"   "+c
        with open(path, "a") as f:
            f.write(atomposition+"\n")
        myposition2.append(atomposition)
    return myposition2
def printenergy(a=molecule):
    """Function to print the potential, kinetic and total energy."""
    epot = a.get_potential_energy() / len(a)
    ekin = a.get_kinetic_energy() / len(a)
    print('Energy per atom: Epot = %.3feV  Ekin = %.3feV (T=%3.0fK)  '
          'Etot = %.3feV' % (epot, ekin, ekin / (1.5 * units.kB), epot + ekin))
    Z=molecule.get_positions()
    m=('Energy per atom: Epot = %.3feV  Ekin = %.3feV (T=%3.0fK) '
                'Etot = %.3feV' % (epot, ekin, ekin / (1.5 * units.kB), epot + ekin)+"\n")
    storexyz(noatom,Z,m)
    return
dyn = Langevin(molecule, 1 * units.fs, 300 * units.kB, 0.2)  #The temperature is changeable
dyn.attach(printenergy, interval=50)
print("Beginning dynamics...")
mydata=printenergy()
dyn.run(10000)
```

APPENDIX B

Extracting Data and Dihedral Calculator using Python (SPYDER)

```
import numpy as np
import math
L=[]
frame={}
framecount = 0
linecount = 0
with open (r'C:\Users\Nurul\Desktop\FYP\Data\TADF in Zeonex\MD\300\acrxtnzero-5-300.txt') as f:
    for line in f:
        L.append(line)
for  line in L:
    findframe = line.find("Energy")
    #use 'frame' for QMD
    #use 'Energy' for MD
   if findframe != -1:
        lineA = linecount + 107
        lineB = linecount + 102
        lineC = linecount + 88
        lineD = linecount + 87
        valueA = L[lineA]
        valueB = L[lineB]
        valueC = L[lineC]
        valueD = L[lineD]
        valueA = valueA.split()
        valueB = valueB.split()
        valueC = valueC.split()
        valueD = valueD.split()
```

```
            A = valueA [1:]
            B = valueB [1:]
            C = valueC [1:]
            D = valueD [1:]
            frame[framecount] = {"A" : A, "B" : B, "C" : C, "D" : D}
            framecount += 1
    linecount += 1
with open (r'C:\Users\300.csv', 'a') as f:
    for frame,value in frame.items():
        # f.write("frame" + frame)
        # f.write(value["A"])
        # f.write(value["B"])
        # f.write(value["C"])
        # f.write(value["D"])
        a = value["A"]
        b = value["B"]
        c = value["C"]
        d = value["D"]
        u1=np.array([a[0],a[1],a[2]])
        u2=np.array([b[0],b[1],b[2]])
        u3=np.array([c[0],c[1],c[2]])
        u4=np.array([d[0],d[1],d[2]])
        pA=u1.astype(np.float)
        pB=u2.astype(np.float)
        pC=u3.astype(np.float)
        pD=u4.astype(np.float)
 def calc_dihedral(pA, pB, pC, pD):
            a1 = ((pB[0]-pA[0]),(pB[1]-pA[1]),(pB[2]-pA[2]))
            a2 = ((pC[0]-pB[0]),(pC[1]-pB[1]),(pC[2]-pB[2]))
```

```
    a3 = ((pD[0]-pC[0]),(pD[1]-pC[1]),(pD[2]-pC[2]))
    a1 = a1/np.sqrt(np.dot(a1,a1))
    a2 = a2/np.sqrt(np.dot(a2,a2))
    a3 = a3/np.sqrt(np.dot(a3,a3))
    v1 = np.cross(a1, a2)
    v2 = np.cross(a2, a3)
    dihedral = math.acos(np.dot(v1,v2))
    return dihedral
alpha = calc_dihedral(pA,pB,pC,pD)
beta = alpha*180/np.pi
f.write("\n" + str(beta))
```

APPENDIX C

Plotting Histogram (Probability Density) Graph of Dihedral Angle Against Temperature Using Python

```
import pandas as pd
import matplotlib.pyplot as plt
import seaborn as sns
#Open file for MD
x1 = pd.read_csv(r'C:\Users \300.csv')
x3 = pd.read_csv(r'C:\Users \T400.csv')
x5 = pd.read_csv(r'C:\Users \T500.csv')
x7 = pd.read_csv(r'C:\Users \T600.csv')
#Open file for QMD
x2 = pd.read_csv(r'C:\Users\T300.csv')
x4 = pd.read_csv(r'C:\Users\T400.csv')
x6 = pd.read_csv(r'C:\Users \T500.csv')
x8 = pd.read_csv(r'C:\Users\ T600.csv')
#Plot a histogram of probability density graph
sns.distplot(x1['Dihedral_angle'], bins = 50, norm_hist = False, hist = False, color ='b')
sns.distplot(x2['Dihedral_angle'], bins = 50, norm_hist = False, hist = False, color = 'g')
sns.distplot(x3['Dihedral_angle'], bins = 50, norm_hist = False, hist = False, color = 'r')
sns.distplot(x4['Dihedral_angle'], bins = 50, norm_hist = False, hist = False, color = 'c')
sns.distplot(x5['Dihedral_angle'], bins = 50, norm_hist = False, hist = False, color ='y')
sns.distplot(x6['Dihedral_angle'], bins = 50, norm_hist = False, hist = False, color = 'm')
sns.distplot(x7['Dihedral_angle'], bins = 50, norm_hist = False, hist = False, color = 'brown')
sns.distplot(x8['Dihedral_angle'], bins = 50, norm_hist = False, hist = False, color = 'k')
plt.legend(['300 K (QMD)','300 K (Full QMD)','400 K (QMD)','400 K (Full QMD)',
        '500 K (QMD)','500 K (Full QMD)','600 K (QMD)','600 K (Full QMD)'])
plt.title('Probability Density against Dihedral Angle'+'\n'+' in QMD Accelerated by Machine
Learning and Full QMD')
plt.xlabel('Dihedral Angle (r'$\theta\degree)$')
plt.ylabel('Probability Density')
```

APPENDIX D

Plotting Mode Values Against Temperature for Full QMD and Machine Learning Accelerated QMD

```
import matplotlib.pyplot as plt
import numpy as np
#QMD
X =np.array([300,400,500,600])
Y =np.array([96,96,79,90])
#MD
X1 =np.array([150,200,250,300,350,400,450,500,600])
Y1 =np.array([75,79,79,81,90,88,80,89,99])
# Mean X1 and Y1
mean_x = np.mean(X1)
mean_y = np.mean(Y1)
n = len(X1)
numer = 0
denom = 0
for i in range(n):
    numer += (X1[i] - mean_x) * (Y1[i] - mean_y)
    denom += (X1[i] - mean_x) ** 2
m = numer / denom
c = mean_y - (m * mean_x)
print("Coefficients")
print(m, c)
# Plotting Values and Regression Line
max_x = np.max(X1) + 100
min_x = np.min(X1) - 100
# Calculating line values x and y
x = np.linspace(min_x, max_x, 1000)
y = c + m * x
plt.plot(x, y, color='b', label = 'Machine Accelerated QMD Regression Plot')
plt.scatter(X, Y,color='r', label = 'Full QMD')
```

```
plt.scatter(X1, Y1, color='b', label ='Machine Accelerated QMD Scatter Plot')
plt.title('QMD Simulations Mode Versus Temperature')
plt.xlabel('Temperature (K)')
plt.legend(['ML QMD Regression Plot','Full QMD','ML QMD Scatter Plot'])
plt.ylabel('Dihedral Angle('r'$\theta\degree)$')
plt.show()
```